Wear 368-369 (2016) 267–277

Contents lists available at ScienceDirect

Wear

journal homepage: www.elsevier.com/locate/wear

Lubricated sliding wear of SAE 1045 and SAE 52100 steel against alumina in the presence of biodiesel, diesel and a 50:50 blend of those fuels

Victor Velho de Castro [a], Luiz Antonio Mazzini Fontoura [b], Juliano Dornelas Benfica [a], Marcus Seferin [a], Joyson Luiz Pacheco [a], Carlos Alexandre dos Santos [a,*]

[a] Pontifícia Universidade Católica do Rio Grande do Sul – PUCRS, Av. Ipiranga, 6681, 90619-900, Porto Alegre, Rio Grande do Sul, Brazil
[b] Fundação de Ciência e Tecnologia do Rio Grande do Sul - CIENTEC, Cachoeirinha, Rio Grande do Sul, Brazil

ARTICLE INFO

Article history:
Received 4 July 2016
Received in revised form
26 September 2016
Accepted 29 September 2016
Available online 1 October 2016

Keywords:
Wear
Pin-on-disk
Steels
Biodiesel
Diesel

ABSTRACT

The purpose of this work was to evaluate the sliding wear characteristics of SAE 1045 and SAE 52100 steels with different microstructures in the presence of pure biodiesel, a biodiesel-diesel blend (50% diesel+50% biodiesel) and commercial diesel fuel. Non-lubricated tests (dry) were also performed for comparison. For SAE 1045, samples were given a hardening heat treatment (austenitization at 830 °C and water quenching). For SAE 52100, the heat treatment was austenitization at 850 °C followed by oil quenching. Tempering at 100 °C and 300 °C was used for SAE 1045, and tempering at 100 °C and 200 °C was used for SAE 52100. As a result, the samples had four different hardness and microstructure combinations: tempered martensite in SAE 1045 and tempered martensite with chromium carbides in SAE 52100. Wear testing was performed using a pin-on-disk tribometer, 1.8 m/s sliding speed, 14.7 N load and 4400 m sliding distance following the ASTM G99-04 standard. Wear track surfaces were characterized using microindentation hardness and scanning electron microscopy. The results exhibited a tendency to decrease wear width, volume loss and wear coefficient when adding biodiesel to diesel for both SAE 1045 and SAE 52100 steels. Martensite produced by heat treatments increased the wear resistance. For both SAE 1045 and SAE 52100 steels, abrasive wear is dominant in both dry and lubricated conditions.

1. Introduction

Biodiesel is a biofuel composed of fatty esters produced by the transesterification of triglycerides or esterification of fatty acids. Several oils and fats can be used as feedstocks. In Brazil, soybean oil and tallow have been the most commonly used material, and transesterification is the main process. In addition to the fatty material, an alcohol, normally methanol, and a catalyst are also utilized [1,2]. Compared to diesel, biodiesel has several advantages. It is made from renewable materials, and it is biodegradable. It has higher flash point, lubricity, and cetane number. In addition, biodiesel is free from sulfur compounds and contributes less to the greenhouse effect [3]. Since 2014, the Brazilian government has adopted the addition of 7% biodiesel in fossil diesel according to the National Program for Production and use of Biodiesel, or PNPB, which began in 2004 with the addition of 2% biodiesel. Biodiesel blends are denoted as "BX," with "X" representing the percentage of biodiesel added to the diesel.

Today, there is a great effort to ensure that vehicles and engine owners utilizing diesel and biodiesel do not suffer any loss of performance due to use of this biofuel [4,5]. One of the major preoccupations of automotive companies is related to the wear of metallic components that are in direct contact with biodiesel. This concern is increasing due to reduction of sulfur content in the fossil diesel, which acts as a lubricity agent. Due to its higher lubricity, biodiesel can minimize this problem when added to diesel [6].

Despite numerous published studies that evaluate wear and friction characteristics using different methods and devices such as pin-on-disc, four-ball, high-frequency reciprocating ring [7–12], just a few studies have investigated the influence of biodiesel on wear behavior of different metallic materials.

A study of the friction and wear characteristics of palm biodiesel was performed by Fazal et al. [13] using a four-ball wear test, different diesel-biodiesel blends (pure diesel, pure biodiesel, and 10%, 20% and 50% biodiesel added to diesel), and speed variations. In this study, they used a chrome alloy steel with a Rockwell hardness of 62 HRC. It was concluded that biodiesel showed better surface protection when compared to fossil diesel. The authors attributed this performance to the surfactant behavior that

* Corresponding author.
E-mail address: carlos.santos@pucrs.br (C.A. dos Santos).

http://dx.doi.org/10.1016/j.wear.2016.09.026
0043-1648/

biodiesel presents due to its ester molecules that are absorbed by the metal surface, permitting the formation of a lubricating film. Similar results were obtained by Habibbullah et al. [6] using four-ball tribometers and biodiesel produced from *Calophyllum inophyllum*, which was added in different concentrations to diesel. A fixed speed of 1800 rpm and carbon-chromium SKF steel with 62 HRC hardness was tested and the best result was obtained for pure biodiesel. In these mentioned papers, friction and wear characteristics were related to friction coefficients, wear scar diameter and surface analysis via scanning electron microscopy (SEM). Farias et al. [14] analyzed the lubricity of different mixtures of diesel and biodiesel using the High Frequency Reciprocating Test Rig (HFRR). They used SAE 52100 steel samples with different hardness values (average ranges of 585 to 677 $HV_{0.2}$ for balls and 174 to 190 $HV_{0.2}$ for discs) in association with complementary techniques such as scanning electron microscopy (SEM), atomic force microscopy (AFM), and microroughness. They reported that pure biodiesel (B100) and diesel-biodiesel blends (B5 and B20) presented better lubricity when compared to fossil diesel, probably due to the better formation of interfacial lubricant film. The wear and friction behavior of Si_3N_4-based ceramic material was reported in the literature [5] using a reciprocating ball-on-plate tribometer. Tests were performed with commercial diesel, biodiesel produced from soybean oil in the laboratory, and a commercial soybean biodiesel from Shell. The results showed that Si_3N_4 presents mild to very mild wear characteristics and that different biodiesels present different lubricating conditions. Nicolau et al. [15] established a relationship between lubricity and electrical impedance in diesels with low sulfur (100 ppm) and high sulfur (130 ppm) fuels, as well as in diesel-biodiesel blends (1%, 3%, 5% and 10%), by determining the wear scar diameter in HFRR tests and the electrical impedance response in a potentiostat coupled with a conductivity cell. A linear correlation was achieved between lubricity and resistivity for diesel mixtures, in addition to an exponential correlation for diesel-biodiesel blends. According to the authors, however, this later correlation is unable to provide a direct relationship to lubricity.

The literature has shown many studies on the effect of biodiesel on standard metallic materials with high chromium content. The effect of chemical composition, microstructures and hardness of steels on wear characteristics, however, has not been reported. The objective of this work is to evaluate the wear characteristics of SAE 1045 and SAE 52100 steels in the presence of pure biodiesel (100% soybean biodiesel), a biodiesel-diesel blend (50% diesel+50% soybean biodiesel), and Brazilian commercial diesel (diesel+7% biodiesel) using a pin-on-disc tribometer. The aim is to analyze the compatibility of SAE 1045 and SAE 52100 steels with different physical-chemical properties of diesel-biodiesel blends. These steels were selected because they are the most important steels used in moving engine components that are in contact with fuels, such as bearings, valves, connecting rods, gears, cylinders, and pistons. The test conditions were chosen in order to permit the analysis of wear characteristics only in the disc (steels) such that an alumina pin with higher hardness was selected to reduce its wear to a minimum and avoid adhesive wear between disc and pin.

2. Materials and methods

2.1. Samples preparation

Samples were machined from commercial SAE 1045 and SAE 52100 hot-rolling steel bars with diameters of 120 mm. Discs with a thickness of 20 mm were cut from bars and initially characterized by optical microscopy for microstructure analyzes. Hardness measurements were taken using the Rockwell method and chemical composition was evaluated using optical emission spectrometry (OES, SpectroMaxx). Table 1 shows chemical compositions of the analyzed steels; the values are an average of three measurements for each material.

Table 1
Chemical compositions of SAE 1045 and SAE 52100 steels (wt%).

Material	Fe	C	Si	Mn	Cr	Mo	Ni
SAE 1045	97.90	0.46	0.280	0.810	0.097	0.018	0.087
SAE 52100	96.30	1.01	0.270	0.390	1.590	0.025	0.074

After initial characterization, discs were heat-treated using the following method: SAE 1045 – austenitization at 850 °C for 30 min and quenching in water, tempering at 100 °C and 300 °C for 30 min and cooling in air; SAE 52100 – austenitization at 850 °C for 30 min and quenching in oil, tempering at 100 °C and 200 °C for 30 min and cooling in air. Fig. 1 shows curves for the tempering conditions of SAE 1045 and SAE 52100 steels as a function of tempering temperatures. All the discs were fully hardened along the thickness.

Both steels are used in the mechanical components of engines and pumps. SAE 1045, a medium carbon steel, is used in shafts, crankshafts, rods, screws, nuts, bolts, and washers, usually in heat-treated conditions, and has a hardness in the range of 40–55 HRC. SAE 52100 steel, known as bearing steel, is a high carbon-chromium steel and is used in bearings, ball bearings, roll bearings, valves, and piston rings, with a hardness between 60 and 62 HRC in the heat-treated conditions.

Before wear tests, discs were machined to a 112 mm diameter and ground on both faces with #100, #220, #320, #400, #600, #1200 sand papers, resulting in a superficial roughness of 0.8 μm. One face was dedicated to dry tests and another face to lubricated tests. Before each test, the discs were cleaned in an ultrasonic bath for 10 min using ethanol, then dried using a hot air hand-held device. After each wear test (in dry and lubricated conditions), discs were machined on both faces in order to remove 2 mm of material in each side, and the surface preparation method was repeated.

2.2. Pin-on-disc apparatus

Within the range of allowable specimens defined in ASTM G-99-04, the balls used were alumina (> 96% Al_2O_3) with diameter of 10 mm [17]. The sliding path is a circle on the disk surface with a 100 mm diameter. The pin-on-disc apparatus contains a loaded pin with weight that provides the normal force that acts on the horizontal disc. An electronic micro controller controls the speed (rpm) and the accumulated sliding distance (m) until a desired number of revolutions is achieved. A 14.7 N load was applied with a sliding speed of 1.8 m/s and a sliding distance of 4400 m in all tests. These conditions were chosen in order to simulate low stress, high-speed contacts, low temperatures and high life cycle in the disc. Fig. 2 shows a schematic representation of the pin-on-disc apparatus and a disc detail image.

2.3. Wear analyses

The wear track width (mm) and volume loss (mm^3) were analyzed for each 400 m sliding distance in 8 locations positioned 45° from each other, as shown in Fig. 3a. All wear track widths were examined using an optical microscope (Fig. 3b) with a measurement system with a resolution of 0.01 mm.

Using Eqs. (1) and (2), it was possible to determine the disc

volume loss (V_{disc}) and the wear coefficient (k) [17]:

$$V_{Disc} = 2\pi R\left[r^2 sen^{-1}\left(\frac{w}{2r}\right) - \frac{w}{4}\left(4r^2 - w^2\right)^{\frac{1}{2}}\right] \quad \left(mm^3\right) \tag{1}$$

$$k = \frac{HB \ x \ V_{Disc}}{P \ x \ L} \quad \left(mm^3/Nm\right) \tag{2}$$

where R is the wear track radius (mm), r is the pin end radius (mm), w is the wear track width (mm), HB is the Brinell hardness, P is the normal applied load (kgf), and L is the sliding distance (mm). As the pin material is harder than the disc material, no significant pin wear was observed after the tests. Additionally, a new pin was used for each test. When the pin wear is insignificant and the ratio of wear track width/sphere radius is < 0.3, the approximate geometric relationship considered in Eq. (1) is correct to 1% [17].

Analyses were performed with pure biodiesel (B100), a biodiesel-diesel blend (B50), commercial Brazilian diesel (diesel with 10 ppm sulfur and 7% of added biodiesel – B7) and in dry conditions. With the exception of the commercial diesel (B7), the biodiesel was obtained via the transesterification process with ethanol, sodium hydroxide, and refined commercial soybean oil. The purification method used water and filtration by 0.5 μm filter paper. The fatty acid ethyl esters (FAEE) of the pure biodiesel were evaluated in accordance with the EN 14103 standard [18], and the results showed 96.4%. The B50 blend was verified by infrared spectrometer (InfraSpec TM VFA-IR, EB) [19], and the fatty acid ethyl ester content was 48.6%.

Each test was performed three times to ensure repeatability, and after each test, the lubricant was filtered through 0.5 mm paper filter in order to avoid contamination. This methodology was applied in order to preserve the same fuel characteristics during test replication. All tests were performed at room temperature (25 °C) and the temperature of the lubrication was monitored with a type J thermocouple immersed in the liquid, which showed a maximum variation of 1 °C during all tests.

2.4. Microstructure and hardness analyses

For metallography analyses, according to ASTM E3 recommendations [20], discs were cut in transversal sections and the specimens were ground with #100, #220, #320, #400, #600, #1200 sand papers, then polished with a 1 μm and 0.5 μm alumina suspension. A Nital 2% solution was used to reveal the microstructures. An optical microscope (Olympus, PMG) was used to obtain metallography images and a scanning electron microscope (SEM-FEG, Inspect F50) was used to analyze wear tracks.

Hardness measurements were taken using the Rockwell method [21], and these values were converted to Brinell values in order to determine the wear coefficient (k) in Eq. (2). Micro Vickers hardness measurements [22] were performed inside and

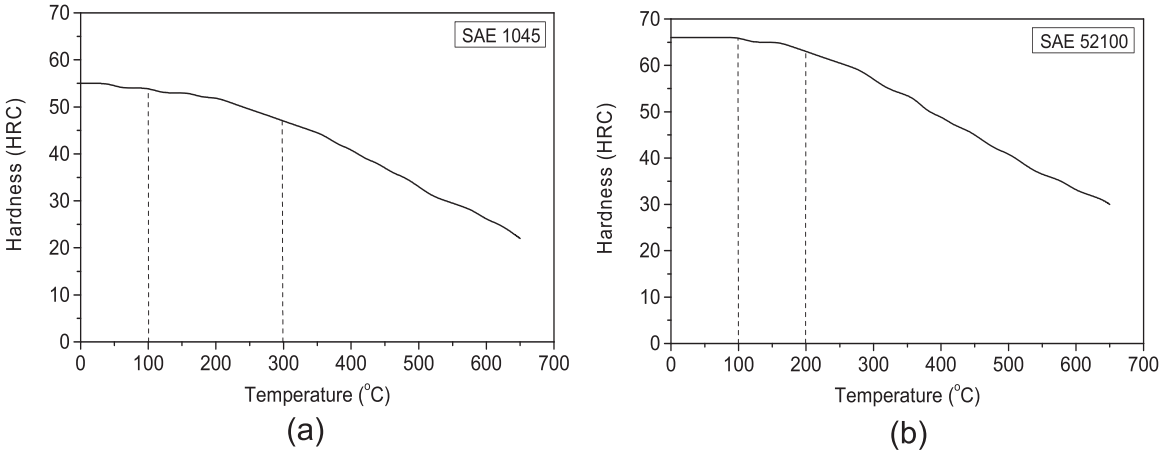

Fig. 1. Tempering curves: (a) SAE 1045 steel, (b) SAE 52100 steel [16].

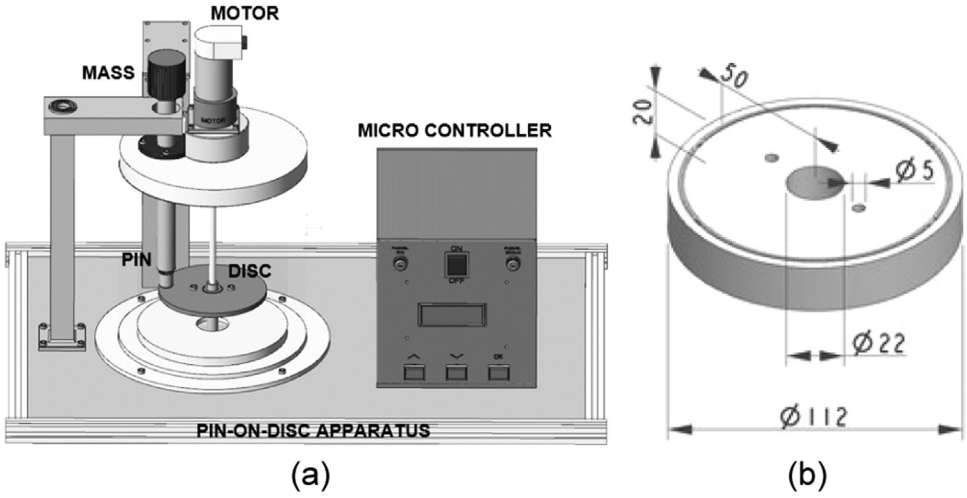

Fig. 2. (a) Schematic representation of the pin-on-disc apparatus, and (b) disc detail.

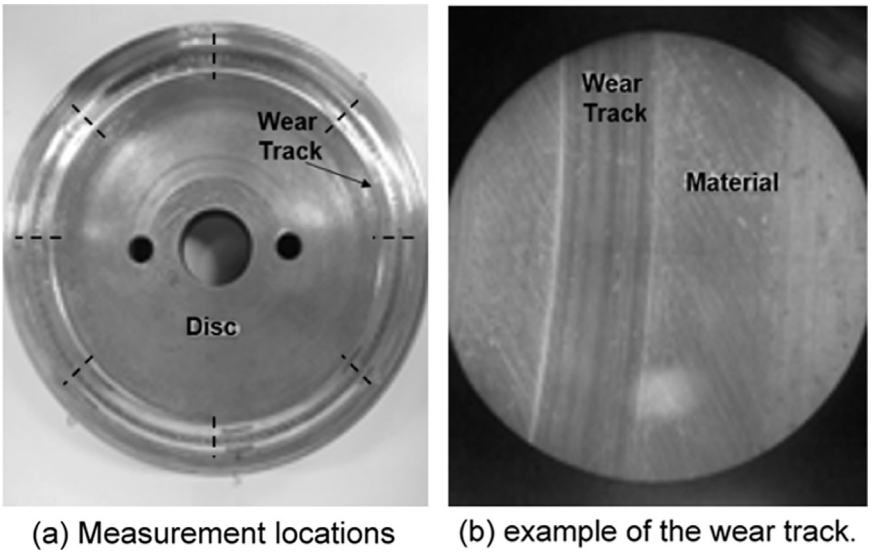

Fig. 3. (a) Measurement locations, and (b) example of the wear track.

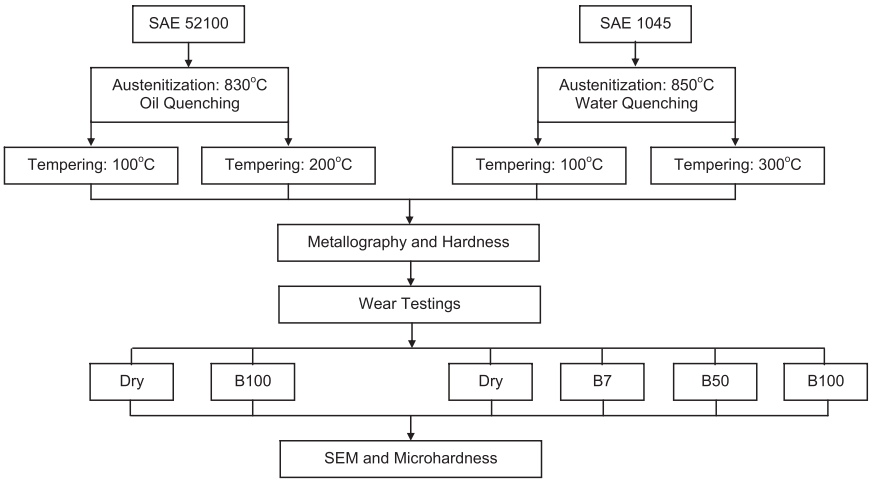

Fig. 4. Flowchart of the experimental procedure.

outside the wear track to determine the strain-hardening of the material after tests (increase in the hardness tracks). The steps of the global applied methodology are presented in Fig. 4.

3. Results and discussion

3.1. Microstructures

Fig. 5 shows the microstructures obtained for the SAE 1045 (left side) and SAE 52100 (right side) steels in the as-received material (before heat treatments), and after quenching and tempering heat treatments. SAE 1045 steel showed a typical microstructure composed of ferrite (light phase) surrounding colonies of lamellae pearlite (Fig. 5a) in the as-received material. After quenching and tempering at 100 °C, microstructures were formed predominantly by tempered martensite with some bainite (Fig. 5b), and at 300 °C the tempered martensite becomes coarser (Fig. 5c). In all samples, it is possible to observe non-metallic inclusions (dark circles) dispersed in the matrix.

SAE 52100 steel showed a typical spheroidized microstructure with cementite (dark globules) and fine chromium carbides (white globules) dispersed in a ferritic matrix (Fig. 5d) in the as-received material. After heat treatments, SAE 52100 showed microstructures composed of tempered martensite with globular chromium carbides. For tempering at 100 °C (Fig. 5e), martensite is finer than that tempered at 200 °C (Fig. 5f), and carbides are similar for both tempering temperatures.

3.2. Hardness

Table 2 shows Rockwell C hardness values obtained for all conditions. These values are the average of six measurements for each sample. For the as-received material, the values were measured on the Rockwell B scale and converted to Rockwell C due to low values. Comparing heat-treated conditions, it is observed that the highest values were obtained for SAE 52100 in both temperatures, with a difference of approximately 2 to 3 points compared to SAE 1045.

According to tempering curves presented in Fig. 1, the values were slightly higher than those suggested by steelmaking catalog [16], probably due to tempering times, which was 30 min in this work and not 60 min as recommended by the steelmaking.

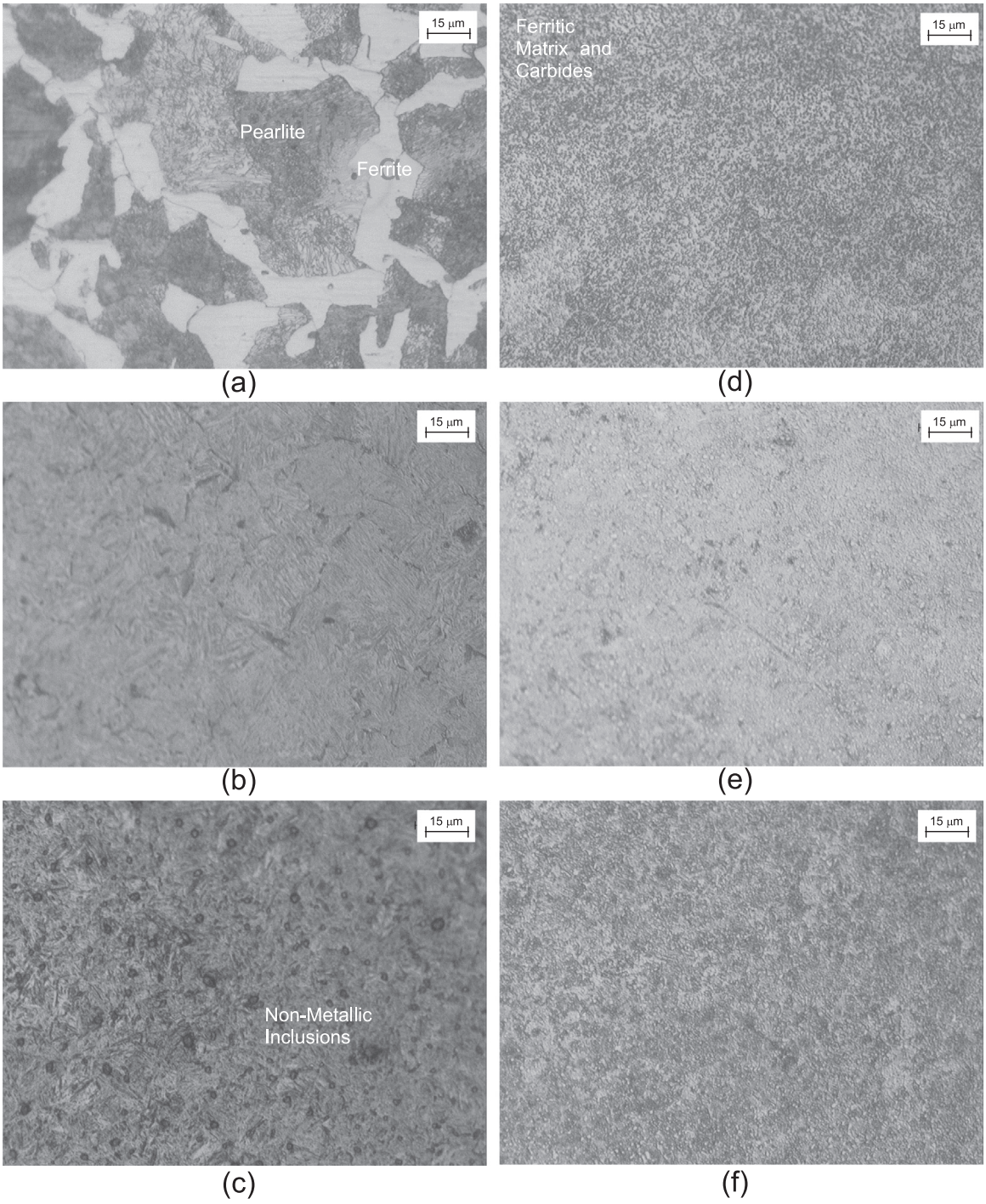

Fig. 5. Microstructures: (a)–(c) SAE 1045 steel, and (d)–(f) SAE 52100 steel.

Table 2
Rockwell C hardness obtained for all conditions.

Steel SAE 1045	As-received 11	Tempering at 100 °C 61	Tempering at 300 °C 52
Steel SAE 52100	As-received 13	Tempering at 100 °C 64	Tempering at 200 °C 54

3.3. Wear track width

The samples for SAE 1045 with three different microstructures and hardnesses were tested in four lubricated conditions: dry, B100, B50, and B7 (Brazilian commercial diesel). Wear track widths are shown in Fig. 6 (mean value and standard deviation of three results).

As can be noted in Fig. 6a, for SAE 1045 in the dry condition, the highest wear track width is observed for the as-received material during all sliding distances; the microstructure is composed of ferrite and pearlite with a hardness of approximately 11 HRC. With the heat treatment and consequent phase transformation to martensite, the wear track width decreases as the hardness increases. The behavior is similar during all sliding distances for both tempering temperatures with average hardness values of 52 HRC and 61 HRC at 300 °C and 100 °C tempering temperatures, respectively.

Analyzing as-received SAE 1045 steel in the presence of

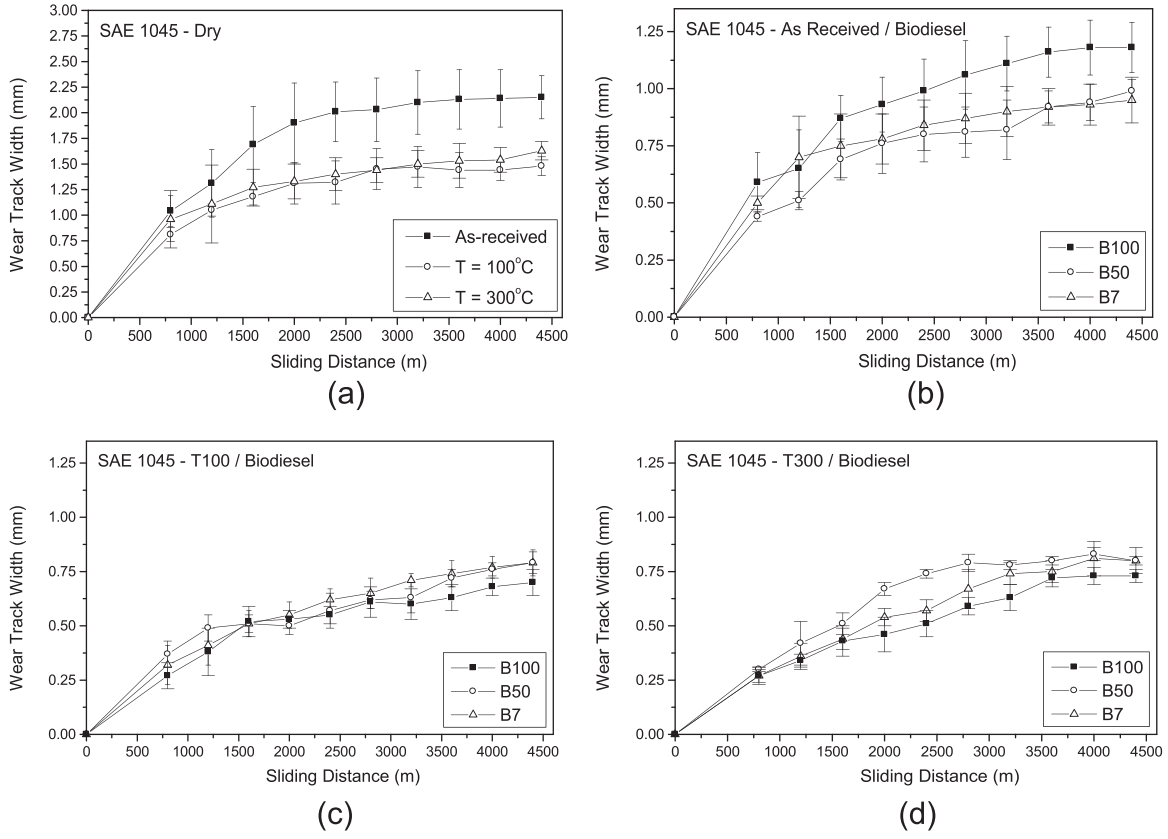

Fig. 6. Wear track width for SAE 1045 steel: (a) dry condition, (b) as-received and lubricated, (c) tempered at 100 °C and lubricated, and (d) tempered at 300 °C and lubricated.

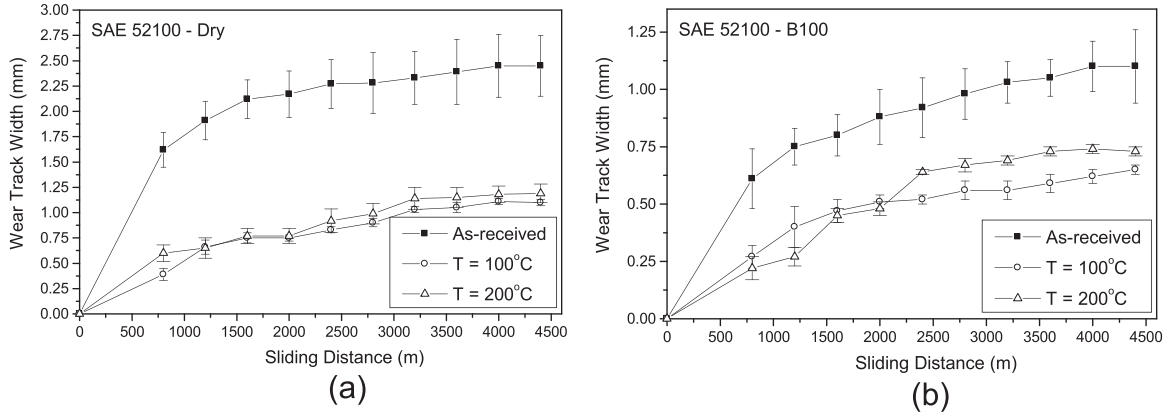

Fig. 7. Wear track width for SAE 52100 steel: (a) dry condition, (b) lubricated with B100.

biodiesel (Fig. 6b), the lowest wear track width is observed for B50, followed by B7 and B100, which presented similar values. In the heat-treated materials, however, the opposite behavior is noted, and the lowest width wear track is attributed to B100, followed by B50 and B7 for tempering at 100 °C (Fig. 6c). After increasing the tempering temperature to 300 °C (Fig. 6d), the behavior of B7 and B50 is changed after 1500 m, probably due to the lower hardness of the tempered martensite and consequently irregular plastic deformation until 4000 m, where the values become almost the same.

In all curves presented in Fig. 6, it is possible to determine two regimes: the first is the transient wear regime and the second is the steady-state wear regime. In the initial transient wear regime, the wear track increases quickly with the sliding distance in a non-linear curve, indicating a high wear rate. After this regime, a linear relationship between wear track width and sliding distance is observed, representing the beginning of the steady-state wear regime [6,8]. In the dry condition, the regime transition was observed at 2500 m for the as-received material and 1600 m for heat-treated materials. Using biodiesel, the transition decreases for both as-received and heat treated steel, as well as from B7 to B100. These results are in agreement with those presented by Fazal et al. [13], which concluded the presence of biodiesel or biodiesel blends can promote alteration from an unsteady-state regime to a steady-state regime due to the interaction of biodiesel with the metal surface.

In the case of SAE 52100 steel, the samples with three different microstructures and hardnesses were tested in two conditions:

dry and lubricated with B100, and the results are presented in Fig. 7. As observed, similar behavior is noted for the material in both dry conditions and with B100, where the highest wear track width is observed for as-received material (spheroidized microstructure), followed by quenched conditions at 200 °C and 100 °C. For dry condition, an identical behavior is noted between 100 °C and 200 °C. This behavior is altered in the presence of B100, however, where a lower quenching temperature, which has a higher hardness, presented lower wear track width.

Comparing both steels in dry conditions, it is observed that as-received SAE 1045 steel showed lower wear track width (2.0 mm) than SAE 52100 steel (2.50 mm), probably due to the different microstructures: in the former there are ferrite and pearlite, and in the latter there are globule carbides in a ferrite matrix. The presence of colonies of pearlite avoids the plastic deformation of ferrite during sliding, while a ferritic matrix in the SAE 52100 steel can deform plastically without limitation. After heat treatments, however, SAE 52100 shows the best behavior in relation to wear for both dry and lubricated conditions.

Based on these results, it is interesting to note that B100 presented the lowest values for wear track width, and consequently, a higher lubricity than B50 and B7. Similar results were reported in the literature by Almeida et al. [5], Farias et al. [14], and Habibullah et al. [6], all of which used SAE 52100 steel as the pattern material in the presence of different diesel and biodiesel blends.

3.4. Wear coefficients and variation in the hardness track

The values of the wear coefficients and hardness track variations after wear tests are presented in Fig. 8 for SAE 1045 steel. In dry tests, the wear coefficient presented the lowest value for material in the as-received condition, followed by heat-treated materials at 100 °C and 300 °C. This behavior can be attributed to the microstructure, composed of ferrite and pearlite for the as-received condition (Fig. 5a), which is softer than tempered martensite, presenting lower values for wear coefficient despite a higher loss volume. With heat treatment and the martensite formation, the higher the microstructure hardness, the lower the wear coefficient.

When biodiesel content increases from B7 to B50, the behavior is similar to the dry condition; however, wear coefficient values are significantly lower. The opposite behavior is noted for B100, where material with heat treatments showed lower wear coefficients compared to the as-received condition. When analyzing variations of hardness inside and outside the tracks, the tendency for an increase in strain-hardening with increasing biodiesel content from dry to B100 for the as-received material is observed. The lowest strain-hardening was observed in the dry condition, probably because the surface material was removed from the track due to severe abrasive wear observed in this case. B7 presented the highest value, and this behavior can be attributed to the plastic deformation of ferrite and pearlite. With the use of B50 and B100, and consequently better lubricity, strain-hardening was slightly lower, although higher than in the dry condition. In the heat treated materials, whose microstructures consist of tempered martensite, as shown in Fig. 5b and c, the behavior is the opposite: strain-hardening decreases as the biodiesel content increases. This variation is more severe for tempering at 100 °C, which presented higher hardness values than tempering at 300 °C (Table 2).

Fig. 9 shows the obtained wear values for SAE 52100 steel. Wear coefficients for the dry condition were higher than those observed for B100 in all microstructures. For the as-received material with a microstructure composed of a ferritic matrix and dispersed globule carbides (Fig. 5d), the wear coefficient was the highest, and decreased sharply with the use of pure biodiesel. For heat-treated materials, wear coefficients decrease slightly for both temperatures, and the use of pure biodiesel showed the lowest value for both temperatures.

Regarding the increase in the hardness track, higher values were observed for as-received material, followed by tempered material at 100 °C and 200 °C, respectively. The highest value for as-received material is due to the microstructure's composition of ferrite and carbides, where the ferrite is in a ductile and soft phase, permitting high strain-hardening. Strain-hardening increased with the use of biodiesel for all conditions, including microstructures side by side with tempered martensite (Fig. 5e and f). Similar to SAE 1045 steel, the highest values were observed for material austempered at 100 °C, with higher hardness in comparison with material austempered at 200 °C.

3.5. Wear track surfaces analyses

Fig. 10 shows worn surface characteristics for as-received SAE 1045 steel obtained by SEM-FEG microscopy in both dry and lubricated conditions. For the dry condition, it is possible to see parallel traces (micro cut) and regions where material was removed from the surface, indicating severe abrasive wear [7,12]. Delamination and debris are also observed, as well as significantly plastic deformation. In the lubricated condition, the material showed mainly micro cuts and scratches for B7. Grooves, delamination, craters in the locations of non-metallic inclusions and corrosive wear in these craters were observed for B50. For B100, the main aspects were grooves and delamination. Because there is no metallurgical compatibility between the pin (Al_2O_3) and the disc (steel), the adhesive wear mechanism was not observed in all conditions [23].

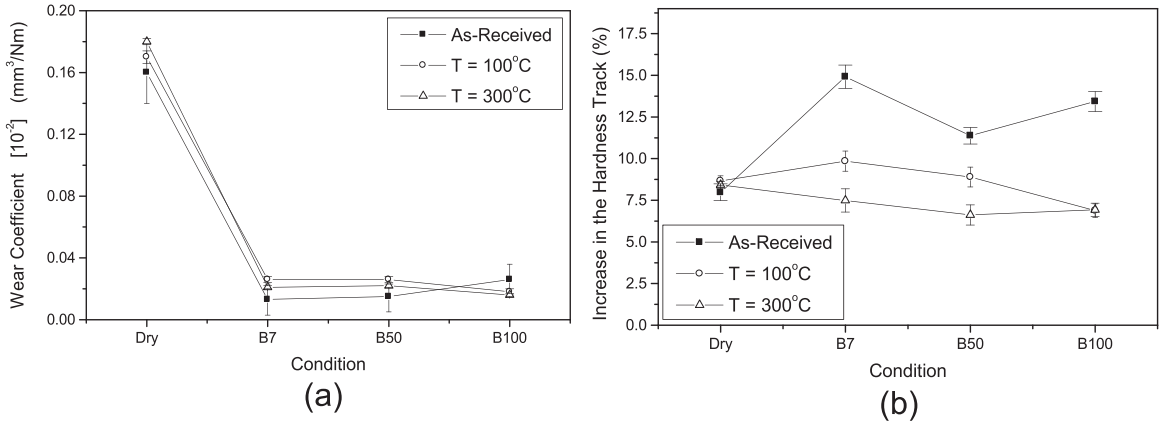

Fig. 8. (a) Wear coefficient for SAE 1045 steel, (b) increase in the hardness track for SAE 1045 (mean value and standard deviation).

According the results, the dry condition presented higher wear damage, probably due to the microstructure being composed of ferrite and pearlite, soft structures. Consequently, it had a higher susceptibility to plastic deformation, strain hardening and fragile behavior. This combination induces material removal, mainly in these regions where there is an interface between ferrite and pearlite. When lubrication is used and wear coefficient decreases, wear damage is reduced in the matrix and the defects are observed mainly in microstructural defects such as non-metallic inclusions and phase interfaces.

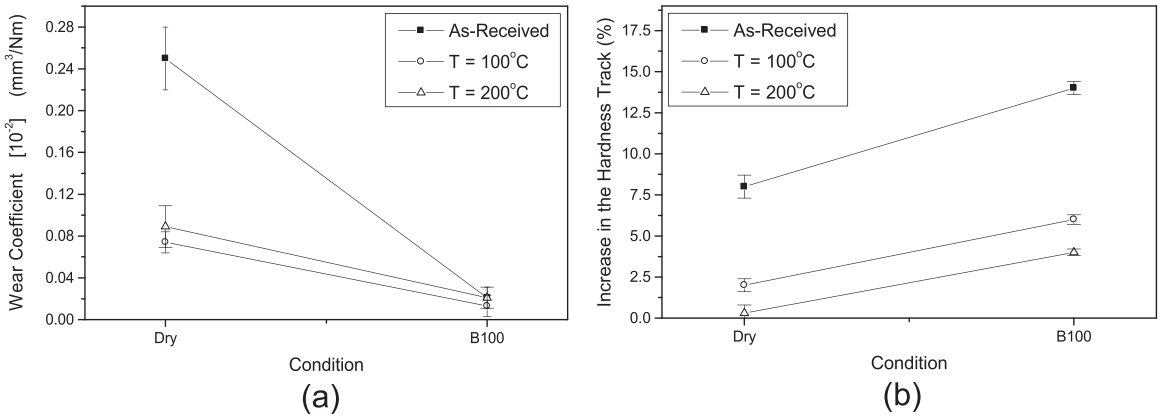

Fig. 9. (a) Wear coefficient for SAE 52100 steel, (b)increase in the hardness track for SAE 52100 (mean value and standard deviation).

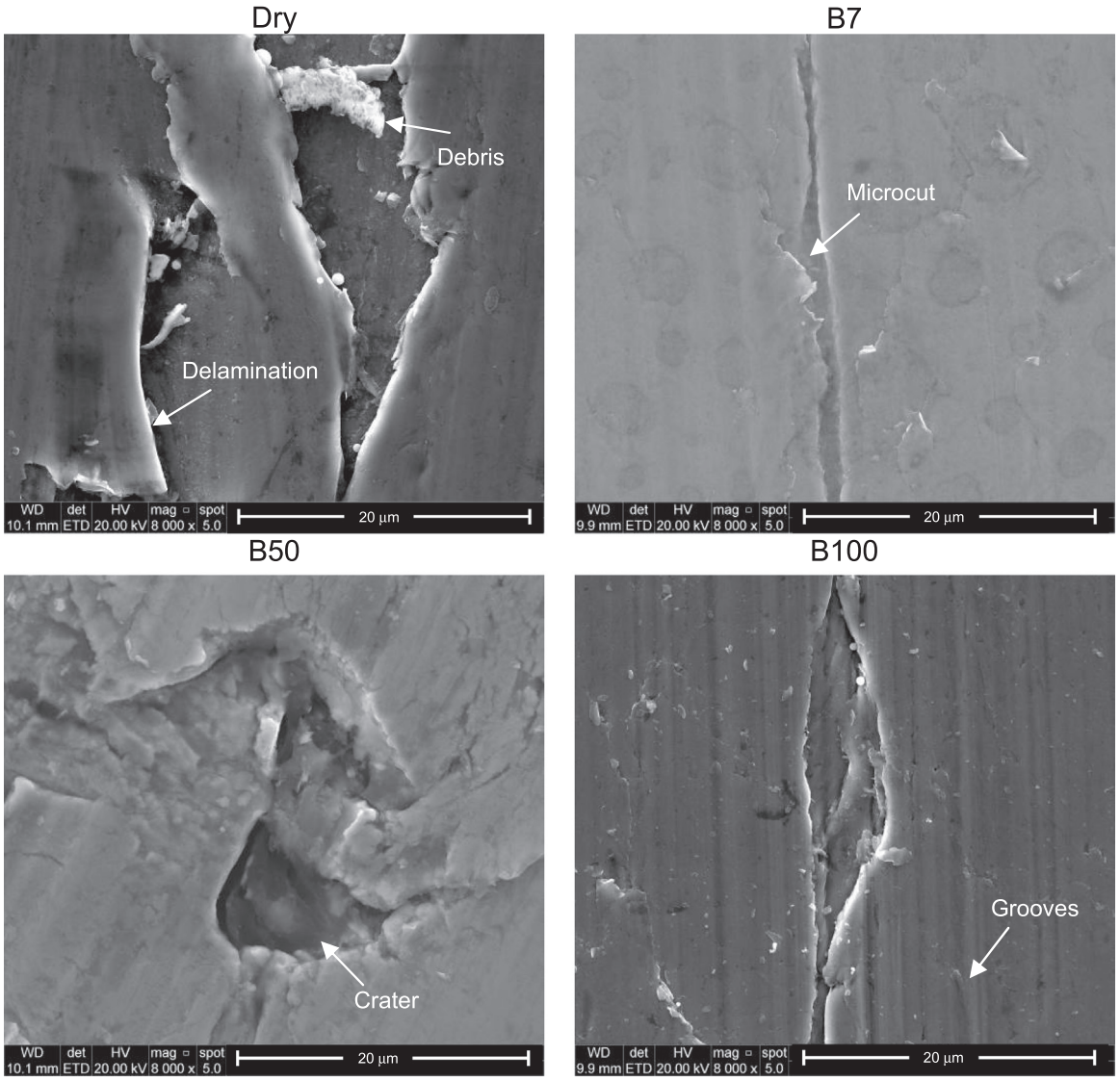

Fig. 10. Wear track surface analyses for SAE 1045 in the as-received condition.

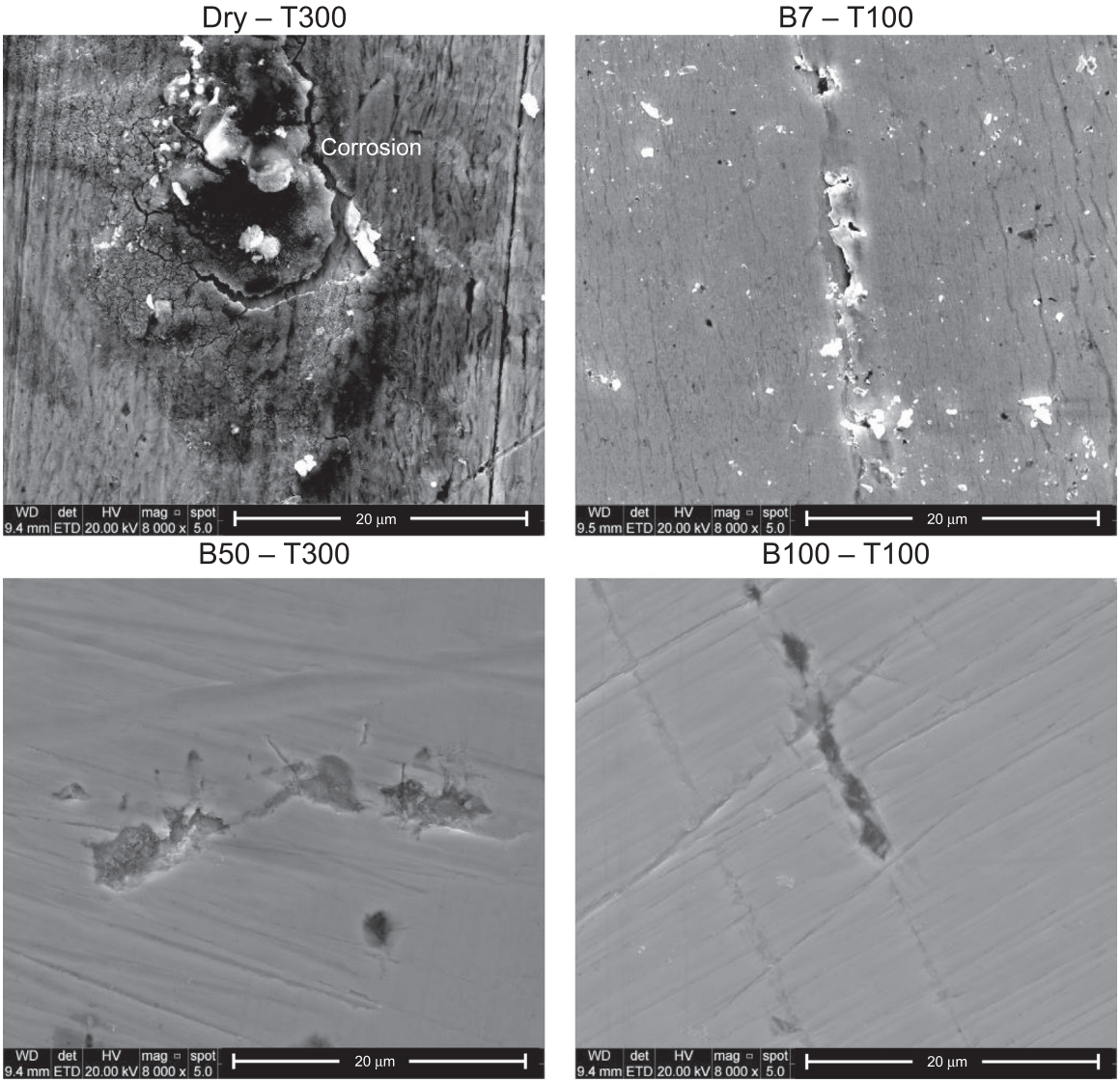

Fig. 11. Wear track surface analyses for SAE 1045 in the heat-treated conditions at 100 °C and at 300 °C.

After heat treatments, materials at both tempering temperatures showed scratches, grooves, craters and plastic deformation indicating that moderate wear damage occurred [11], as shown in Fig. 11. Corrosion (Fig. 11a) and detached material are also observed in some areas (Fig. 11b) in both tempering temperatures, probably due to contact between fragments formed during sliding with non-metallic inclusions dispersed in the matrix and the consequent crater formation [9]. After increasing biodiesel to B50 and B100, wear damage decreased and only craters were observed for both tempering conditions (Fig. 11c and d). In comparison with wear track width, heat-treated materials showed lower values than as-received materials mainly in the steady-state wear regime, despite the higher wear coefficients. This behavior can be attributed to the higher tempered martensite matrix hardness, which decreases the probability of abrasion when compared to the softer ferrite and pearlite matrix. For all heat-treated materials, the predominant wear mechanism is abrasive, with some craters in the location of non-metallic inclusions.

Micrographs of worn surface characteristics for SAE 52100 are shown in Fig. 12. In the dry condition for as-received material, samples showed wear debris, galling and regions with plastic deformation, indicating severe abrasive wear conditions. Comparing both steels, the wear coefficient is higher for SAE 52100 (0.25×10^{-2} mm^3/N m) than SAE 1045 (0.16×10^{-2} mm^3/N m) and is probably due to the soft ferritic matrix in the case of SAE 52100, where dispersed carbides do not protect the matrix [9]. This is also noted with the use of B100, where the matrix was worn and the carbides remained unaltered. In the case of SAE 1045 steel, colonies of pearlite are homogenously distributed in the ferritic matrix and the abrasive wear in the ferrite regions is minimized.

For heat-treated materials, surfaces presented some grooves and small and concentrated craters in the dry condition, probably due to the removal of carbides from the tempered martensite matrix. These carbides act as hard particles that plow the material of the matrix. In the presence of B100, tempered martensite with higher hardness showed better behavior when tempered at 100 °C than when tempered at 200 °C. In both cases, the wear mechanism is abrasive, with presence of grooves, scratches and craters.

From the obtained results, it is possible to note that the higher amount of biodiesel added to diesel led to lower wear damage. This behavior is influenced, however, by the material micro-

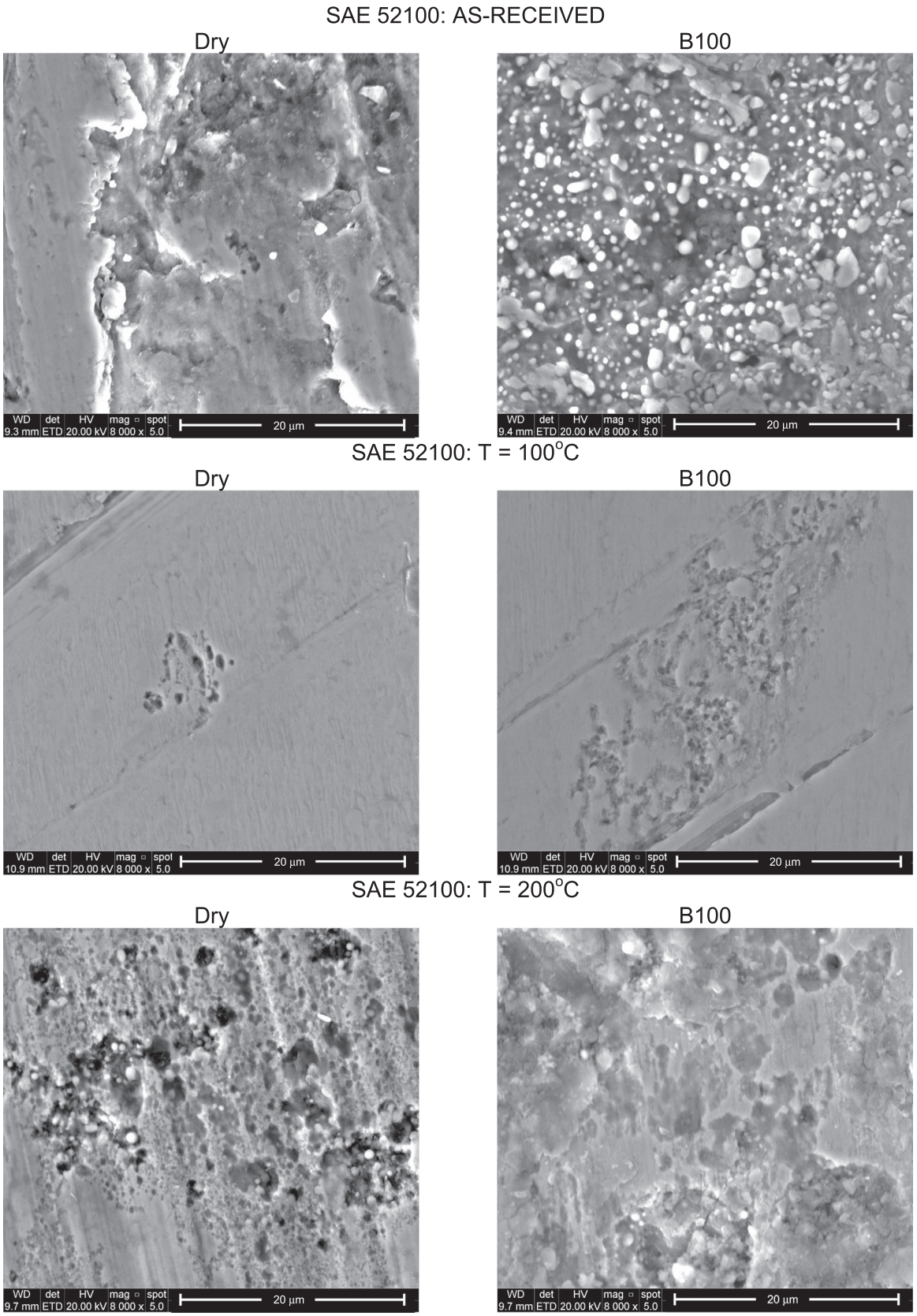

Fig. 12. Wear track surface analyses for SAE 52100.

structures that are created by manufacturing processes. The results demonstrated that the tempered martensite microstructure had better wear resistance in the presence of biodiesel in comparison to the ferrite-pearlite microstructure. This behavior is more pronounced in the case of SAE 52100. With higher biodiesel content, damage wear was decreased for both steels, indicating that lubricity in terms of friction and wear decreases compared to B7 [24]. These tests provided useful and important information on

the effect of diesel-biodiesel blends on the wear characteristics of SAE 1045 and SAE 52100 steels, permitting insights into the pre-programming of material conditions in terms of microstructures, heat treatments and mechanical properties.

4. Conclusions

Experiments were conducted to analyze the evolution of the wear characteristics of SAE 1045 and SAE 52100 steels in presence of diesel and biodiesel, as well as without lubrication (dry). The following conclusions can be drawn:

- Under dry conditions and with as-received microstructures, SAE 1045 steel presented lower wear damage than SAE 52100 steel. This is probably due to the uniform distribution of pearlite colonies surrounding the ductile ferrite in the SAE 1045 that protects matrix wear, while in SAE 52100, the ductile ferritic matrix is not protected by dispersed carbides. After heat treatments, however, SAE 52100 steel shows lower wear damage when compared to SAE 1045 steel in the presence of dispersed carbides in SAE 52100, which help to protect the tempered martensite matrix.
- In the lubricated tests for SAE 1045 steel, the best wear resistance was observed with B100, followed by B50 and B7 in the case of the tempered martensite microstructure. In the presence of ferrite and pearlite microstructures, the opposite was true, with the highest wear resistance observed with B7, followed by B50 and B100.
- For SAE 52100, the use of B100 decreased sharply wear damage for both as-received and heat treated materials.
- Because the pin material is harder than disc material, no significant pin wear was observed.
- In all conditions, the observed wear mechanism was abrasive wear.

Acknowledgments

The authors would like to thank CNPq (Grant no. 067/2008) (The Brazilian Research Council – Project RHAE – Researcher in the Company), FINEP (Project MCT/FINEP/CT-PETRO/PROMOPETRO-PROMOBIO – 02/2009) and FAPERGS (State Foundation for Research of Rio Grande do Sul) for their financial support.

References

[1] A.C. Pinto, L.L. Guarieiro, M.J.C. Rezende, N.M. Ribeiro, E.A. Torres, W.A. Lopes, P.A.P. Pereira, J.B. Andrade, Biodiesel: an overview, J. Braz. Chem. Soc. 16 (2005) 1313–1330.
[2] L.C. Meher, D.V. Sagar, S.N. Naik, Technical aspects of biodiesel production by transesterification, Renew. Sustain. Energy Rev. 10 (2006) 248–268.
[3] G. Knothe, "Designer" biodiesel: optimizing fatty ester composition to improve fuel properties, Energy and Fuels, vol. 22, 2008, pp.1358–1364.
[4] M.A. Fazal, A.S.M.A. Haseeb, H.H. Masjuki, Biodiesel feasibility study: an evolution of material compatibility; performance; emission and engine durability. Renewable and Sustainable Energy Reviews, vol. 15, 2011. pp.1314–1324.
[5] F.A. Almeida, M.M. Maru, L.N. Batista, F.J.A. Oliveira, R.R.F.S. Silva, C.A. Achete, Wear and friction behaviour of Si_3N_4 ceramics under diesel and biodiesel lubrication, J. Mater. Res. Technol. 2 (2013) 110–116.
[6] M. Habibullah, H.H. Masjuki, M.A. Kalam, N.W.M. Zulkifli, B.M. Masum, A. ARSLAN, M. GULZAR, Friction and wear characteristics of Calophyllum inophyllum biodiesel, Ind. Crop. Prod. 76 (2015) 188–197.
[7] L.J. Yang, Wear coefficient of tungsten carbide against hot-work tool steel disc with two different pin settings, Wear (2004) (vol. 257, p. 481 – 231).
[8] L.J. Yang, A test methodology for the determination of wear coefficient, Wear 259 (2005) 1453–1461.
[9] G.A. Fontalvo, R. Humer, C. Mitterer, K. Sammt, I. Schemmel, Microstructural aspects determining the adhesive wear of tool steels, Wear 260 (2006) 1028–1034.
[10] S. Syahrullail, N. Nuraliza, M.I. Izhan, M.K. Abdul Hamid, D.M. Razaka, Wear characteristic of palm olein as lubricant in different rotating speed, Procedia Eng. 68 (2013) 158–165.
[11] Y. Lyu, Y. Zhu, U. Olofsson, Wear between wheel and rail: a pin-on-disc study of environmental conditions and iron oxides, Wear 328–329 (2015) 277–285.
[12] X. Li, M. Sosa, U. Olofsson, A pin-on-disc study of the tribology characteristics of sintered versus standard steel gear materials, Wear 340–341 (2015) 31–40.
[13] M.A. Fazal, A.S.M.A. Haseeb, H.H. Masjuki, Investigation of friction and wear characteristics of palm biodiesel, Energy Convers. Manag. 67 (2013) 251–256.
[14] A.C. Farias, J.T.N. Medeiros, S.M. Alves, Micro- and nanometric wear evaluation of metal discs used on determination of biodiesel fuel lubricity, Mater. Res. 17 (2014) 89–99.
[15] A. Nicolau, C.V. Lutckmeier, D. Samios, M. Gutterres, C.M.S. Piatnick, The relation between lubricity and electrical properties of low sulfur diesel and diesel/biodiesel blends, Fuel 117 (2014) 26–32.
[16] Gerdau Special Steels – Catalog, 2014. ⟨www.ggdmetals.com.br/aco-especiais⟩, ⟨www.ggdmetals.com.br/aco-construcao-mecanica⟩.
[17] ASTM G99 – 04, Standard test method for wear testing with a pin-on-disk apparatus, Am. Soc. Test. Mater., ASM Society, United States, 2004, 5 p.
[18] EN 14103, Fats and oil derivatives – fatty acid methyl esters (FAME) – determination of ester and linolenic acid methyl esters contents, European Standard, European Committee for Standardization, Belgium, 2003, 18p.
[19] ASTM D 7371-12, Standard test method for determination of biodiesel (fatty acid methyl esters) content in diesel fuel oil using mid infrared spectroscopy (FTIRATR- PLS Method), Am. Soc. Test. Mater., ASM Society, United States, 2012, 10p.
[20] ASTM E3 – 11, Standard guide for preparation of metallographic specimens, Am. Soc. Test. Mater., ASM Society, United States, 2011, 8p.
[21] ASTM E18-03, Standard test methods for Rockwell hardness and Rockwell superficial hardness of metallic materials, Am. Soc. Test. Mater., ASM Society, United States, 2004, 22p.
[22] ASTM E384 – 99, Standard test method for microindentation hardness of materials, Am. Soc. Test. Mater., ASM Society, United States, 2000, 24p.
[23] G.W. Stachowiak, A.W. Batchelor, Engineering Tribology, 3th edition, Elsevier Butterworth Heinemann, Boston, 2005.
[24] A.S.M.A. Haseeb, S.Y. Sia, M.A. Fazal, H.H. Masjuki, Effect of temperature on tribological properties of palm biodiesel, Energy 35 (1464) (2010) 1460.